Bioorganic Chemistry 89 (2019) 102974

Contents lists available at ScienceDirect

Bioorganic Chemistry

journal homepage: www.elsevier.com/locate/bioorg

Follow on-based optimization of the biphenyl-DAPYs as HIV-1 nonnucleoside reverse transcriptase inhibitors against the wild-type and mutant strains

Yali Sang[a,b], Sheng Han[a,b], Shuwen Han[a,b], Christophe Pannecouque[c], Erik De Clercq[c], Chunlin Zhuang[a,b], Fener Chen[a,b,*]

[a] Engineering Center of Catalysis and Synthesis for Chiral Molecules, Department of Chemistry, Fudan University, Shanghai 200433, People's Republic of China
[b] Shanghai Engineering Center of Industrial Asymmetric Catalysis for Chiral Drugs, Shanghai 200433, People's Republic of China
[c] Rega Institute for Medical Research, KU Leuven, Herestraat 49, B-3000 Leuven, Belgium

ARTICLE INFO

Keywords:
HIV-1
Biphenyl
Thiophene [3,2-*d*] pyrimidines
DAPYs
Reverse transcriptase

ABSTRACT

The present work follows our preliminary discovery of biphenyl diarylpyrimidines (DAPYs) as HIV-1 nonnucleoside reverse transcriptase inhibitors. Further structural optimization of biphenyl-DAPYs led to the identification of a new series of biphenyl-substituted thiophene[3,2-*d*]pyrimidine analogues by a scaffold-hopping strategy. Biological evaluation of this series showed that these compounds possessed up to single-digit nanomolar potency (EC_{50} = 7.8–526.2 nM) and prominently low toxicity (CC_{50} = 18.5–280.8 μM) against wild-type (WT) HIV-1-infected cells. Furthermore, the results also demonstrated that compounds **29–32** exhibited high, broad-spectrum antiviral effects against clinically observed HIV-1 mutants. Specifically, compound **30**, which had the highest selectivity index (SI = 16094) and the best anti-reverse transcriptase ability (IC_{50} = 39 nM), displayed marked inhibitory activity (EC_{50} = 13.5, 9.4, 17.0, 52.0, and 58.2 nM) against WT, K103N, E138K, L100I, Y181C mutants and moderate activity against double mutants. This study provides important avenues for the further design of HIV-1 inhibitors.

1. Introduction

In our continuous studies of novel HIV-1 nonnucleoside reverse transcriptase inhibitors (NNRTIs) [1–5], we recently identified a series of biphenyl-DAPY derivatives with low nanomolar antiviral activity against HIV-1 wild-type strains and a panel of NNRTI-resistant single and double mutant strains [6]. It was noteworthy that the inhibitory ability of the most potent compound **1** was 1.8–5.4-fold greater against L100I, K103N, E138K, and Y181C compared with ETV. Other variants of biphenyl derivatives have also been explored as HIV-1 inhibitors (Fig. 1). Wang and coworkers described a report on a novel series of 2-hydroxyisoquinoline-1,3-dione (HID, **2**) with dual inhibitory activity, which consistently inhibited HIV reverse transcriptase (RT)-associated RNase H and polymerase with IC_{50} values in low to submicromolar range [7]. Guillemont et al. developed DAPY analogues **3** with different spacer groups G (e.g., 2-furyl heterocycle, alkenyl group, etc.) between the cyano moiety and the phenyl ring that displayed substantially potent inhibitory capacity against the panel of the mutant virus. The structure-activity relationship (SAR) studies illustrated that the spacer group G in **3** maximized the interaction with the NNRTI binding pocket (NNIBP) by extending the length of the π-π conjugated system to improve the potentially antiviral activity [8]. Liu and his colleagues synthesized a series of new DAPYs **4** with longer and bulkier alkyne groups in the left wing (e.g., aromatic ring, cycloalkane, etc.), and the newly synthesized compounds showed significantly better antiviral profiles because of the beneficial effects of the extensive interactions between the extended left ring and the functional residues in the hydrophobic tunnel [9]. Despite the above advantages of these variants, the related toxicity and/or unfavorable selectivity index (SI) has particularly limited the potential for further drug development, and the present study has raised concerns around these serious problems.

The previous reports from the Liu group indicated that thiophene [3,2-*d*]pyrimidine could be a useful architecture for DAPY-type agents with significant inhibitory activity toward resistance-associated HIV-1 variants [10,11]. In particular, these compounds exhibited good safety with low toxicity and high SI values. Our previous work also demonstrated that a fused aromatic core (e.g., benzopyrimidine ring) could strengthen the van der Waals interaction between compounds and the

* Corresponding author.
E-mail address: rfchen@fudan.edu.cn (F. Chen).

https://doi.org/10.1016/j.bioorg.2019.102974
Received 25 March 2019; Received in revised form 16 April 2019; Accepted 4 May 2019
Available online 04 May 2019
0045-2068/

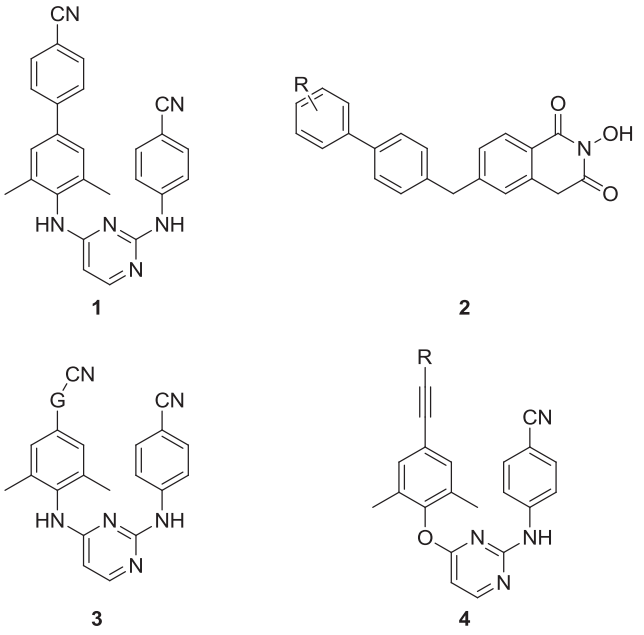

Fig. 1. DAPY lead **1** and variants of biphenyl derivatives.

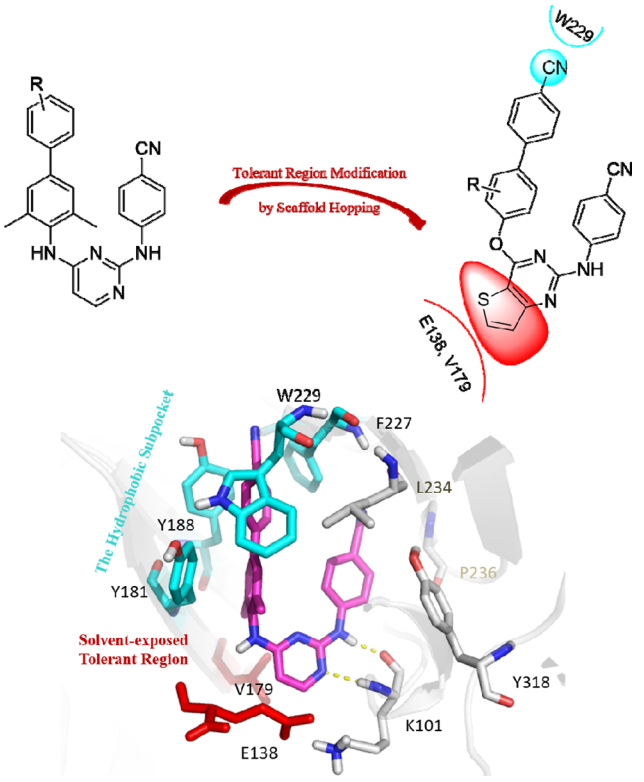

Fig. 2. Illustration of the optimization strategy to develop new biphenyl-DAPY analogues.

adjacent residues (e.g., E138, V179, etc.) in NNIBP [12]. These derivatives with fused rings adjacent to the solvent-exposed tolerant region (the largely open region in front of K103, E138, and V179) not only improved the anti-HIV-1 potency but also reduced the potential risk of cytotoxicity with high SI values. In the present work, we further assembled a thiophene ring into the biphenyl-DAPYs by a scaffold-hopping strategy to address current disadvantages of anti-HIV drugs (Fig. 2). The present pharmacophore involves additional electrostatic interactions between the thiophene[3,2-*d*]pyrimidine structure and

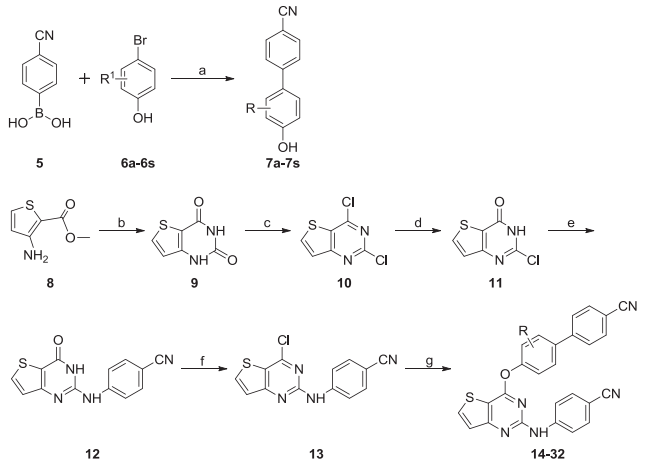

Scheme 1. Synthesis of compounds **14–32.** [a]Reagents and conditions: (a) $PdCl_2$, K_2CO_3, PEG_{400}, H_2O, 25 °C, 5–24 h; (b) urea, 190 °C, 2.5 h; (c) $POCl_3$, DMF (*cat.*), 110 °C, 8 h; (d) (i) NaOH, THF, H_2O, 50 °C, 4 h. (ii) AcOH, 35 °C, 2 h; (e) 4-Aminobenzonitrile, EtOH, N_2, 85 °C, 12 h; (f) $POCl_3$, 110 °C, 2 h; (g) **7a-7s**, K_2CO_3, DMF, 80 °C, 8 h.

functional residues V179 and E138 to increase the specificity of these counterparts toward HIV-1 RT.

In drug discovery, building strong interactions of the analogues with conserved regions of the NNIBP is a widely accepted strategy to enhance the anti-RT potency of NNRTIs [13–15]. The Dousson group demonstrated that a polar cyano group specially interacting with the highly conserved residue, W229, is particularly beneficial to improve mutant resilience [16]. Therefore, a cyano group is selected as a key component in this framework with the hope to improve the binding affinities of the biphenyl-DAPYs. The resistance profiles of these new compounds against HIV-1 wild-type and prevalent drug-resistant mutant variants are further evaluated in this article.

2. Results and discussion

2.1. Chemistry

The synthetic route to the desired compounds **14–32** is outlined in Scheme 1. First, the key intermediates, 4′-hydroxy-[1,1′-biphenyl]-4-carbonitrile **7a-7s** were generated by Suzuki-Miyaura cross-coupling reaction of **5** and **6a-6s**. Then, treatment of commercially available methyl 3-aminothiophene-2-carboxylate **8** with urea under the solvent-free conditions generated 1,3-dihydrothiopheno[3,2-*d*]pyrimidine-2,4-dione **9**, which followed by chlorination, hydrolysis and nucleophilic substitution reactions provided the intermediate **13**. Subsequent reaction with the key intermediates **7a-7s** yielded the final compounds **14–32**.

2.2. Antiviral activity

The newly synthesized biphenyl compounds were evaluated for their antiviral potency and cytotoxicity in MT-4 cells infected with WT HIV-1 strain (IIIB), HIV-2 strain (ROD) or a wide range of clinically observed drug-resistant single and double mutant strains (L100I, K103N, E138K, Y181C, Y188L, K103N + Y181C (RES056) and F227L + V106A). The values of the anti-HIV activity (EC_{50}), cytotoxicity (CC_{50}), and selectivity index (SI, CC_{50}/EC_{50} ratio) of the synthesized NNRTI derivatives are illustrated in Tables 1 and 2. The FDA-approved drugs, nevirapine (NVP), efavirenz (EFV), and etravirine (ETV), were selected as reference compounds.

As summarized in Table 1, the biphenyl compounds with a cyano group and a thiophene attached to the pyrimidine exhibited high antiviral activity against the WT HIV-1 (IIIB) strain with submicromolar to

Table 1
Activity and cytotoxicity against HIV-1 (IIIB) and HIV-2 (ROD) strains in MT-4 cells.

Compounds	R	EC_{50}[a]		CC_{50} (μM)[b]	SI (IIIB)[c]
		HIV-1 (IIIB) (nM)	ROD (μM)		
14	H	67.4 ± 22.5	41.1 ± 6.4	> 280.8	> 4151
15	2-Me	54.5 ± 10.5	> 8.7	18.5 ± 5.9	341
16	3-Me	58.8 ± 14.0	56.4 ± 21.1	187.3 ± 45.4	3152
17	2-F	47.5 ± 25.9	> 125.0	> 269.9	> 5580
18	3-F	101.5 ± 41.0	36.5 ± 13.4	> 269.9	> 2682
19	2-Cl	39.7 ± 7.1	> 16.1	33.6 ± 16.1	852
20	3-Cl	229.6 ± 50.5	75.8 ± 26.3	> 261.0	> 1176
21	2-CF_3	54.6 ± 15.6	95.1 ± 43.8	> 243.6	> 4401
22	3-CF_3	526.2 ± 389.8	> 13.6	26.5 ± 5.0	50
23	2-CN	70.2 ± 14.9	≥124.5	> 265.9	> 3744
24	3-CN	76.6 ± 23.0	1.4 ± 0.6	192.1 ± 48.0	2512
25	2-NO_2	7.8 ± 3.7	> 107.2	218.8 ± 37.3	28,346
26	3-NO_2	87.7 ± 30.6	> 34.4	70.2 ± 19.2	803
27	2-OMe	35.8 ± 23.2	57.5 ± 11.3	> 263.1	> 7289
28	3-OMe	25.3 ± 6.8	> 116.9	246.1 ± 6.5	9506
29	2,6-diMe	38 ± 12.7	1.4 ± 0.3	223.8 ± 69.0	5868
30	2,3-diF	13.5 ± 5.6	> 104.3	216.9 ± 6.7	16,094
31	2,6-diF	12.3 ± 2.1	> 37.8	78.6 ± 22.0	6423
32	2-Me-6-Cl	34.5 ± 16.2	> 70.3	142.7 ± 63.4	4144
NVP		309.4 ± 57.7	> 4.0	> 15.9	> 51
EFV		7.3 ± 8.3	> 2.0	> 6.4	> 863
ETV		5.5 ± 4.1	> 2.0	> 4.6	> 833

[a] EC_{50}: The effective concentration required to protect the cell against viral cytopathicity by 50% in MT-4 cells.
[b] CC_{50}: The cytotoxic concentration of the compound that reduces the normal uninfected MT-4 cell viability by 50%.
[c] SI: selectivity index, ratio CC_{50}/EC_{50} (WT).

Table 2
Inhibitory activity of the selected compounds toward WT HIV-1 RT.

Compounds	IC_{50} (nM)[a]	Compounds	IC_{50} (nM)[a]
25	63 ± 12	**31**	41 ± 9
29	44 ± 2	**32**	44 ± 14
30	39 ± 6	**NVP**	404 ± 85

[a] IC_{50}: inhibitory concentration of the test compound required to inhibit biotin deoxyuridine triphosphate (biotin-dUTP) incorporation into WT HIV-1 RT by 50%.

single-digit nanomolar EC_{50} values (EC_{50} = 7.8–526.2 nM). The SAR analysis indicated that (1) the derivatives substituted on position 2 are better than the substituted derivatives on position 3, with only one exception (compound **27**). Compound **25** with 2-nitro group showed the best anti-HIV-1 activity with an IC_{50} value of 7.8 nM. The ortho-substitutions are favorable to the selectivity (SI, ranging from 341 to 28346), with two exceptions (**15** and **19**). (2) Di-substituted compounds exhibit different anti-HIV-1 activity. The di-fluorinated derivatives (**30** and **31**) exhibited EC_{50} values of low nanomolar range. However, di-methyl (**29**) and 2-methyl-6-chloride (**32**) had an approximately 3-fold decrease of anti-HIV-1 compared to the di-fluorinated derivatives, indicating the tolerance of small substitutions on C_6-position. (3) Although these analogues showed comparable or less potency against the WT HIV-1, they had much better selectivity against HIV-1 over ROD (EC_{50} > 3.0–269.9 μM), and their cytotoxicities were much lower (CC_{50} > 18.5–280.8 μM) than the four reference drugs (CC_{50} > 4.6–15.9 μM).

Because good anti-HIV-1 activity, low cytotoxicity and/or high SI of compounds **25** and **29–32** were observed, they were further

Table 3
Activity and selectivity index of the selected compounds against a panel of clinically relevant HIV-1 mutant strains in MT-4 cells.

Compounds	EC_{50} (nM)[a] (SI)[b]						
	L100I	K103N	Y181C	Y188L	E138K	RES056	F227L + V106A
25	18.2 ± 3.9 (12,118)	5.5 ± 0.6 (39,719)	55.1 ± 6.1 (40,039)	> 15140.0 (14)	6.5 ± 0.5 (34,045)	> 218821.4 (1)	≥40911.7 (11)
29	23.2 ± 4.2 (8014)	33.8 ± 4.2 (5318)	57.1 ± 10.6 (3197)	50.7 ± 17.0 (3531)	42.3 ± 4.2 (44,254)	152.2 ± 42.3 (1191)	253.6 ± 8.5 (703)
30	52.0 ± 8.3 (4116)	9.4 ± 2.1 (23,187)	58.2 ± 33.3 (3753)	228.6 ± 41.6 (940)	17.0 ± 0.2 (12,725)	> 2037.1 (106)	602.8 ± 20.8 (354)
31	47.8 ± 8.3 (1615)	8.7 ± 2.7 (9106)	120.6 ± 18.7 (654)	> 20308.0 (4)	16.6 ± 2.1 (4724)	> 78552.4 (11)	≥7233.70 (1)
32	28.4 ± 16.2 (4505)	30.4 ± 6.1 (4079)	48.7 ± 14.2 (2665)	107.5 ± 42.6 (1183)	52.7 ± 6.1 (2418)	148.0 ± 20.3 (854)	405.6 ± 6.1 (314)
NVP	2102.3 ± 751.5 (8)	> 10075.0 (X1)	> 15866.7 (X1)	> 15866.7 (X1)	210.2 ± 26.3 (75)	> 15866.7 (X1)	> 15866.7 (X1)
EFV	44.4 ± 9.5 (140)	101.6 ± 54.0 (63)	7.3 ± 0.6 (870)	292.0 ± 44.4 (22)	6.3 ± 0.6 (1013)	279.3 ± 98.4 (23)	273.0 ± 28.6 (23)
ETV	7.1 ± 2.8 (640)	3.2 ± 0.5 (1429)	12.0 ± 1.4 (388)	20.0 ± 7.6 (231)	6.5 ± 5.8 (721)	55.3 ± 9.2 (83)	15.2 ± 16.1 (302)

[a] EC_{50}: The effective concentration required to protect the cell against viral cytopathicity by 50% in MT-4 cells.
[b] SI: selectivity index, ratio CC_{50}/EC_{50} (mutant strains).

investigated for their inhibitory activity against WT HIV-1 RT enzymes. NVP was chosen as the reference drug. To our delight, the five novel NNRTI derivatives displayed great inhibitory activity against WT HIV-1 RT with IC_{50} values ranging from 39 nM to 63 nM, which were 6.4–10.5-fold higher than that of NVP (IC_{50} = 404 nM) (Table 2).

Then, the five representative compounds were also selected to be evaluated for their efficacy against the HIV-1 mutant strains, bearing the L100I, K103N, Y181C, Y188L, E138K, RES056 (K103N + Y181C) and F227L + V106A mutations that are associated with resistance to NVP and EFV (Table 3).

Overall, they showed low EC_{50} values against most of the mutant variants and much higher SI values than those observed for the positive drugs. Compound **25** bearing a NO_2 group presented prominent inhibitory efficacy (EC_{50} = 18, 5.5, 55.1 and 6.5 nM) against L100I, K103N, Y181C, and E138K mutations, comparable to that of EFA and ETV. Meanwhile, the SI values of **25** against L100I, K103N, Y181C, and E138K mutations (SI = 12,118, 39,719, 40,039 and 34,045) were obviously better than those of all of the references. However, it was inactive to Y188L and double mutant variants RES056 and F227L + V106A. Compound **31** showed a similar profile as compound **25**, which was inactive against the double mutants. Compound **30** was favorable to K103N and E138K (EC_{50} = 9.4 nM and 17.0 nM, respectively) and showed EC_{50} values lower than 1 μM toward double mutant variants RES056 and F227L + V106A. The 2,6-dimethyl-substituted **29** was the most potent inhibitor toward the dual mutant variants RES056 (EC_{50} = 152 nM, SI = 1191) and F227L + V106A (EC_{50} = 253 nM, SI = 703), and it demonstrated similar activity and a similar SI as the 2-methyl-6-chloro-substituted **32**, which were comparable to that of EFV, ETV and better than NVP. Taking the chemical structure into consideration, the methyl group in the di-substituted compounds (**29**, **32**) was positive to the potency against double mutants compared to the difluoro compounds (**30**, **31**).

2.3. Molecular modeling analysis

Molecular docking was performed to explain the binding mode of the representative compound **30** to HIV-1 RT, which has the best activity at enzyme level (Fig. 3A). The docking model possessed similar binding orientation with typical horseshoe conformational shape, consistent with our earlier report on compound **1** (Fig. 3B). The biphenyl group was inserted deeply into the aromatic-rich subpocket, which was composed by hydrophobic amino acid residues Y181, Y188, F227, and W229. Meanwhile, the cyano group became a powerful attachment to a certain conserved region of W229 via extending the length of the π-π conjugated system. The *para*-cyanoaniline group of **30** at the C_2-position of the pyrimidine was essential for antiviral potency by interacting with V106, P236, L100, L234, and Y318, as well as attributing to the hydrogen-bonding interaction with the main chain of the residue K101 as a hydrogen bond donor. Notably, the additional thiophene ring further extended into the solvent-exposed tolerant region and established nonpolar interactions with E138 and V179 residues as expected. Another hydrogen bond between the nitrogen atom of the thiophene [3,2-*d*]pyrimidine and the K101 side-chain was observed. Collectively, these interactions are proposed to have contributed to the binding affinity.

To further elucidate the resistance features of these compounds, molecular models were created for the K103N and E138K variants of the HIV-1 RT (Fig. 4). The binding orientation of compound **30** in complexes with K103N mutant HIV-1 RT was similar to the binding orientation in those with WT-HIV-1 RT (Fig. 3). Differently, a water-mediated hydrogen bond (2.6, 2.2 Å) between the amino hydrogen of N103 and the nitrogen atom in the central pyrimidine ring was formed (Fig. 4A), indicating the contribution to the efficacy against the drug-resistant K103N mutant virus. Consistent with the findings of the Liu group [17], the predicted complex of the E138K RT/**30** complex showed that the Glu to Lys did not impair the electrostatic interactions between the thiophene[3,2-*d*]pyrimidine structure and backbone K138 (Fig. 4B). Compound **30** inserted into the NNIBP as the **30**/WT complex, forming strong hydrophobic interactions with residue K138. As a result, compound **30** retained its potency to this mutation as WT RT.

3. Conclusion

In summary, novel NNRTIs that combine structural features of 4-cyano-1,1′-biphenyl substitutions and the thiophene[3,2-*d*]pyrimidine were synthesized to overcome the high toxicity and improve the potency. Current structural modification analysis indicated that (1) the presence of a cyano group on the biphenyl ring was essential to interact with the highly conserved W229 residue and endowed these derivatives with promising activities and specificity in the wild-type and drug-resistant mutant HIV-1 strains, (2) optimization of the substituents on the biphenyl group could maintain or improve antiviral ability and form an excellent combination of the biological efficiency and cytotoxicity, and (3) the central thiophene[3,2-*d*]pyrimidine ring played a key role in enhancing the specificity of these candidates targeting HIV-1 RT. Overall, the newly designed compounds with tri-substitutions on the biphenyl ring exhibited high broad-spectrum antiviral effects and low cytotoxicity or high SI. This study provides a promising 4-cyano-1,1′-biphenyl thiophene[3,2-*d*]pyrimidine scaffold as the novel lead template for further investigation on anti-HIV-1 agents.

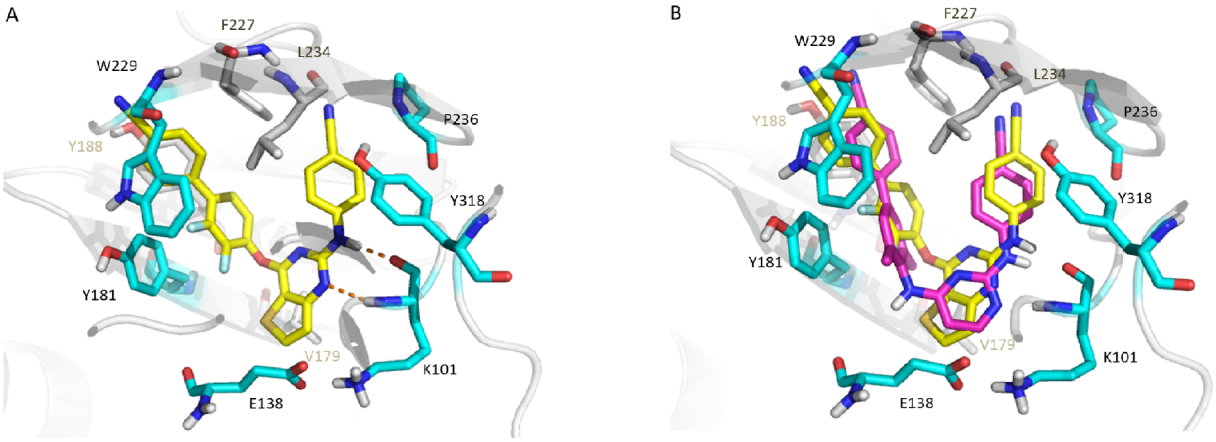

Fig. 3. (A) Predicted binding mode of **30** with the HIV-1 WT RT crystal structure (PDB:2ZD1). (B) Superimposition of **1** and **30** with WT RT (pink, **1**; yellow, **30**). Hydrogen bonds are indicated as orange dashed lines. The figure was generated using PyMol (http://pymol.sourceforge.net/). (For interpretation of the references to color in this figure legend, the reader is referred to the web version of this article.)

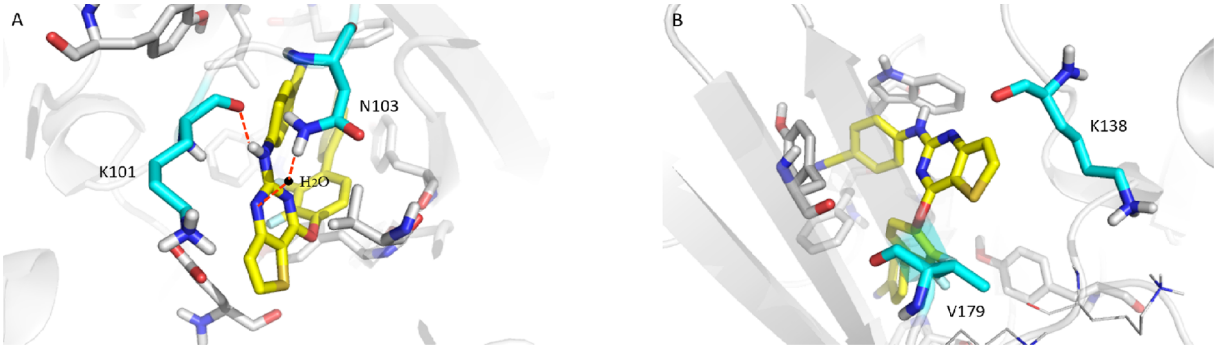

Fig. 4. (A) Predicted binding mode of **30** with the HIV-1 K103N RT crystal structure (PDB: 6C0K). (B) Predicted binding mode of **30** with the HIV-1 E138K RT crystal structure (PDB: 6C0L). Hydrogen bonds are indicated as red dashed lines. The figure was generated using PyMol (http://pymol.sourceforge.net/).

4. Experimental

4.1. General

$POCl_3$ was freshly distilled with an absorption apparatus for tail gas under N_2. EtOH was freshly distilled from Magnesium and iodine under N_2. Unless otherwise specified, all reagents and solvents were purchased from commercial sources and used as received. Flash column chromatography was performed on silica gel (300–400 mesh). Thin-layer chromatography (TLC) carried out on 0.25 mm silica gel platesvisualized with UV light (λ = 254 nm) and/or by staining with ethanolic phosphomolybdic acid (PMA) or iodine. Proton nuclear magnetic resonance (^{1}H NMR) and carbon nuclear magnetic resonance (^{13}C NMR) spectra were recorded in DMSO-d_6 or CF_3COOD, $CDCl_3$ on a Bruker AV-400 spectrometer with tetramethylsilane (TMS) as the internal standard. Chemical shifts (δ) are given in ppm relative to TMS, coupling constants (J) in Hz. Melting points were measured on WRS-1B digital melting-point apparatus. EI-MS were recorded on an Agilent 6890 N/5975 spectrometer and ESI-MS were recorded on a Waters Micromass Quattro Micro spectrometer. High-resolution mass spectra were recorded on Bruker ApeXIII 7.0 TESLA FTMS. The purities of the compounds were analyzed by HPLC (Agilent 1260) using a C18 column (Eslipse XDB, 4.6 * 150 mm, 5 μm) with methanol/water as the mobile phase at a flow rate of 1 mL/min: (a) 0–10 min, 30% MeOH; (b) 10–15 min, 30–60% MeOH; (c) 15–20 min, 60–95% MeOH; (d) 20–35 min, 95% MeOH; (e) 35–37 min, 95–30% MeOH; (f) 37–40 min, 30% MeOH. All final compounds exhibited purities greater than 95%.

4.2. General procedure for the preparation of final compounds *7a-7s*

A reaction mixture of (4-cyanophenyl)boronic acid **5** (150 mg, 1.02 mmol, 1.0 equiv.), 4-bromo-2-chloro-6-methylphenol **6s** (271 mg, 1.22 mmol, 1.2 equiv.) and potassium carbonate (353 mg, 2.55 mmol, 2.5 equiv.) in PEG400/H_20 (4 mL/4 mL) was stirred at room temperature for 15 min, and then $PdCl_2$ (1.8 mg, 0.01 mmol, 0.01 equiv.) was added to it. Stirring was continued for an additional 15 h until complete consumption of starting material as judged by TLC. Then the reaction mixture was poured into water (20 mL) and extracted with ethyl acetate (10 mL * 4). The organic layers were washed with brine, dried over anhydrous Na_2SO_4, filtered and condensed. The residue was then purified via flash chromatography on silica gel, eluting with EtOAc/petroleum ethe to **7s** as white solid in 54% yield. ^{1}H NMR (400 MHz, DMSO-d_6) δ: 9.50 (1H, s), 7.87–7.78 (4H, m), 7.60 (1H, s), 7.49 (1H, s), 2.27 (3H, s). MS (ESI) m/z $C14H_{10}ClNO$: calcd 243.05, found 244.11 $[M + 1]^+$.

The compounds **7a**-**7r** were synthesized following the general procedure, starting from **5** and phenol with different substituents **6a**-**6r**.

4.3. Preparation of *9*

Treatment of commercially available methyl 3-aminothiophene-2-carboxylate **8** (10.0 g, 63.62 mmol, 1.0 equiv.) with urea (19.1 g, 318.09 mmol, 5.0 equiv.) at 190 °C for 2.5 h under the solvent-free conditions generated intermediate thieno[3,2-*d*]pyrimidine-2,4(*1H,3H*)-dione (**9**). Upon cooling to about 90 °C, the reaction mixture was poured into aqueous solution of sodium hydroxide (200 mL, 1 N) slowly. Then the mixture was stirred for 1 h and any insoluble material removed by filtration. The mixture was then acidified by 15% HCl solution until pH was adjusted to 4–5 to yield desired compound **9** as a white precipitate, which was collected by filtration, washed by water and dried. Yield: 92%. ^{1}H NMR (400 MHz, DMSO-d_6) δ: 11.53 (s, 1H), 11.19 (s, 1H), 8.03 (d, J = 5.0 Hz, 1H), 6.91 (d, J = 5.0 Hz, 1H). MS (ESI) m/z $C_6H_4N_2O_2S$: calcd 168.00, found 169.07 $[M + 1]^+$.

4.4. Preparation of *10*

To a solution of intermediates **9** (9.0 g, 53.52 mmol) in phosphorus oxychloride (60 mL) were added a few drops of dimethyl sulfoxide under a nitrogen atmosphere. After the mixture was stirred for 8 h at 105 °C, TLC analysis indicated the reaction was complete. The solvent was removed under reduced pressure and the residue was poured onto ice-water with vigorous stirring yielding a precipitate. The precipitate was then collected by filtration, washed by H_2O and dried to give the intermediates **10** as off-white solid. Yield: 73%. ^{1}H NMR (400 MHz, DMSO-d_6) δ: 8.69 (d, J = 5.4 Hz, 1H), 7.72 (d, J = 5.4 Hz, 1H). MS (ESI) m/z $C_6H_2Cl_2N_2S$: calcd 203.93, found 204.94 $[M + 1]^+$.

4.5. Preparation of *11*

10 (8.0 g, 39.01 mmol, 1.0 equiv.) was dissolved in 80 mL of a mixture solvent of THF and H_2O (4:1), and a solution in which NaOH (3.9 g, 97.53 mmol, 2.5 equiv.) was dissolved in 17 mL of H_2O was added. The resulting mixture was heated to 50 °C and stirred for 4 h. Then the reaction solution was cooled to 40 °C, 4.8 mL of acetic acid was added to the reaction solution and stirred for another 2 h. The resulting white solid was filtered, washed with H_2O and dried to obtain **11** in 89% yield. ^{1}H NMR (400 MHz, DMSO-d_6) δ: 13.47 (s, 1H), 8.17 (d, J = 5.2 Hz, 1H), 7.31 (d, J = 5.2 Hz, 1H). MS (ESI) m/z $C_6H_3ClN_2OS$: calcd 185.97, found 186.92 $[M + 1]^+$.

4.6. Preparation of *12*

A solution of intermediate **11** (6.5 g, 34.83 mmol, 1.0 equiv.) and 4-aminobenzonitrile (4.11 g, 34.83 mmol, 1.0 equiv.) in pure EtOH (65 mL) was stirred at 85 °C for 12 h under N_2 atmosphere. Then the solution was cooled to room temperature and stand for another15 h. The resulting precipitate was collected by filtration, and dried to give crude **12**, which was used directly in the next step without further

purification. MS (ESI) *m/z* $C_{13}H_8N_4OS$: calcd 268.04, found 269.13 $[M + 1]^+$.

4.7. Preparation of **13**

To a solution of intermediate **12** (5.0 g, 18.64 mmol) in phosphorus oxychloride (40 mL) were added a few drops of dimethyl sulfoxide under a nitrogen atmosphere. After the mixture was stirred for 2 h at 105 °C, TLC analysis indicated the reaction was complete. The solvent was removed under reduced pressure and the residue was poured onto ice-water with vigorous stirring. The pH of the solution was adjusted to 7 by 1 N NaOH aqueous solution and the solution was stirred for another 2 h yielding a precipitate. The precipitate was then collected by filtration. The collected solid was stirred in 50 mL of a mixture solvent of acetone and water (4:1), and then filtered to get a white solid **13** in 80% yield. ^{1}H NMR (400 MHz, DMSO-d_6) δ: 10.56 (s, 1H), 8.47 (d, J = 5.1 Hz, 1H), 8.02 (d, J = 8.4 Hz, 2H), 7.76 (d, J = 8.4 Hz, 2H), 7.52 (d, J = 5.2 Hz, 1H). MS (ESI) *m/z* $C_{13}H_7ClN_4S$: calcd 286.01, found 287.16 $[M + 1]^+$.

4.8. General procedure for the preparation of the final compounds **14–32**

Different substituted 4′-hydroxy-[1,1′-biphenyl]-4-carbonitrile (0.2 mmol, 1.0 equiv.) was dissolved in DMF (3 mL) in the presence of K_2CO_3 (0.6 mmol, 3.0 equiv.), followed by addition of the compound **13** (0.2 mmol, 1.0 equiv.). The reaction mixture was stirred at 85 °C for 6–8 h (monitored by TLC), and then the reaction was cooled to ambient temperature and poured into 15 mL H_2O yielding a precipitate. The precipitate was collected by filtration and the residue was then purified via flash chromatography on silica gel, eluting with EtOAc/petroleum ether (1/5, v/v) to obtain **14–32** as white solid.

4.8.1. 4′-((2-((4-Cyanophenyl)amino)thieno[3,2-d]pyrimidin-4-yl)oxy)-[1,1′-biphenyl]-4-carbonitrile (**14**)

Yield: 75%. mp: 274.3–275.8 °C. ^{1}H NMR (400 MHz, DMSO-d_6) δ: 10.06 (s, 1H), 8.38 (d, J = 5.2 Hz, 1H), 7.97 (s, 4H), 7.92 (d, J = 8.5 Hz, 2H), 7.82 (d, J = 8.4 Hz, 2H), 7.55–7.51 (m, 4H), 7.47 (d, J = 5.3 Hz, 1H). ^{13}C NMR (101 MHz, CF_3COOD, $CDCl_3$) δ: 166.76, 151.79, 151.55, 150.52, 144.88, 142.75, 140.33, 138.84, 133.38, 133.16, 129.09, 127.81, 122.34, 121.36, 118.48, 117.54, 117.10, 116.73, 112.83, 110.00, 106.95. HRMS (ESI) *m/z* $C_{26}H_{15}N_5OS$: calcd 445.0997, found 446.1068 $[M + H]^+$. HPLC analysis: retention time = 22.3 min; peak area, 96.8%.

4.8.2. 4′-((2-((4-Cyanophenyl)amino)thieno[3,2-d]pyrimidin-4-yl)oxy)-3′-methyl-[1,1′-biphenyl]-4-carbonitrile (**15**)

Yield: 67%. mp: 261.1–262.5 °C. ^{1}H NMR (400 MHz, DMSO-d_6) δ: 10.10 (s, 1H), 8.38 (d, J = 5.3 Hz, 1H), 7.96 (s, 4H), 7.84 (s, 1H), 7.79–7.74 (m, 3H), 7.50–7.45 (m, 4H), 2.23 (s, 3H). ^{13}C NMR (101 MHz, CF_3COOD, $CDCl_3$) δ: 166.50, 151.55, 150.73, 150.59, 145.13, 142.76, 140.40, 138.87, 133.33, 133.17, 131.32, 130.75, 127.79, 126.51, 122.38, 121.19, 118.53, 117.63, 112.87, 111.31, 110.05, 109.83, 106.85, 15.67. HRMS (ESI) *m/z* $C_{27}H_{17}N_5OS$: calcd 459.1154, found 460.1215 $[M + H]^+$. HPLC analysis: retention time = 22.6 min; peak area, 98.6%.

4.8.3. 4′-((2-((4-Cyanophenyl)amino)thieno[3,2-d]pyrimidin-4-yl)oxy)-2′-methyl-[1,1′-biphenyl]-4-carbonitrile (**16**)

Yield: 83%. mp: 243.9–246.6 °C. ^{1}H NMR (400 MHz, DMSO-d_6) δ: 10.07 (s, 1H), 8.37 (d, J = 5.2 Hz, 1H), 7.95 (d, J = 7.6 Hz, 2H), 7.86 (d, J = 8.3 Hz, 2H), 7.63 (d, J = 7.6 Hz, 2H), 7.56 (d, J = 8.2 Hz, 2H), 7.46 (d, J = 5.2 Hz, 1H), 7.39 (d, J = 8.6 Hz, 2H), 7.32 (d, J = 8.3 Hz, 1H), 2.30 (s, 3H). ^{13}C NMR (101 MHz, CF_3COOD, $CDCl_3$) δ: 166.81, 151.58, 151.16, 150.35, 146.17, 142.62, 140.46, 139.51, 138.20, 133.14, 132.78, 131.04, 129.97, 123.29, 121.49, 119.06, 118.47, 117.45, 112.82, 111.73, 110.00, 109.69, 106.92, 19.88. HRMS (ESI) *m/z* $C_{27}H_{17}N_5OS$: calcd 459.1154, found 460.1217 $[M + H]^+$. HPLC analysis: retention time = 22.5 min; peak area, 95.1%.

4.8.4. 4′-((2-((4-Cyanophenyl)amino)thieno[3,2-d]pyrimidin-4-yl)oxy)-3′-fluoro-[1,1′-biphenyl]-4-carbonitrile (**17**)

Yield: 89%. mp: 290.0–291.2 °C. ^{1}H NMR (400 MHz, DMSO-d_6) δ: 10.12 (s, 1H), 8.44 (d, J = 5.3 Hz, 1H), 8.05–7.99 (m, 5H), 7.80–7.71 (m, 4H), 7.54–7.50 (m, 3H). ^{13}C NMR (101 MHz, CF_3COOD, $CDCl_3$) δ: 165.89, 153.94, 151.71, 150.89, 143.77, 143.14, 140.63, 140.20, 138.92, 133.48, 133.12, 127.74, 123.97, 121.73, 118.40, 117.56, 116.75, 116.03, 115.84, 112.76, 110.60, 109.93, 107.18. HRMS (ESI) *m/z* $C_{26}H_{14}FN_5OS$: calcd 463.0903, found 464.0973 $[M + H]^+$. HPLC analysis: retention time = 22.2 min; peak area, 96.6%.

4.8.5. 4′-((2-((4-Cyanophenyl)amino)thieno[3,2-d]pyrimidin-4-yl)oxy)-2′-fluoro-[1,1′-biphenyl]-4-carbonitrile (**18**)

Yield: 81%. mp: 288.3–290.4 °C. ^{1}H NMR (400 MHz, CF_3COOD, $CDCl_3$) δ: 8.43 (d, J = 5.4 Hz, 1H), 7.96 (d, J = 8.2 Hz, 2H), 7.84 (d, J = 7.9 Hz, 2H), 7.74 (t, J = 8.5 Hz, 1H), 7.59–7.52 (m, 5H), 7.31 (t, J = 8.1 Hz, 2H). ^{13}C NMR (101 MHz, CF_3COOD, $CDCl_3$) δ: 166.36, 159.82, 151.88, 151.77, 151.71, 150.68, 143.06, 140.19, 139.87, 133.20, 132.97, 131.56, 131.52, 129.66, 129.63, 121.84, 118.49, 118.15, 118.11, 117.50, 112.84, 111.60, 110.93, 110.67, 110.36, 110.02, 107.33. HRMS (ESI) *m/z* $C_{26}H_{14}FN_5OS$: calcd 463.0903, found 464.0973 $[M + H]^+$. HPLC analysis: retention time = 22.5 min; peak area, 95.8%.

4.8.6. 3′-Chloro-4′-((2-((4-cyanophenyl)amino)thieno[3,2-d]pyrimidin-4-yl)oxy)-[1,1′-biphenyl]-4-carbonitrile (**19**)

Yield: 68%. mp: 289.4–292.0 °C. ^{1}H NMR (400 MHz, CF_3COOD, $CDCl_3$) δ: 8.43 (d, J = 5.4 Hz, 1H), 8.14 (s, 1H), 8.04 (d, J = 10.0 Hz, 1H), 7.98 (d, J = 8.3 Hz, 2H), 7.88 (d, J = 8.3 Hz, 2H), 7.61 (d, J = 8.5 Hz, 1H), 7.57 (d, J = 5.4 Hz, 1H), 7.44 (q, J = 8.9 Hz, 4H). ^{13}C NMR (101 MHz, CF_3COOD, $CDCl_3$) δ: 165.92, 151.60, 150.92, 147.83, 143.66, 143.18, 140.24, 133.49, 133.10, 129.52, 127.86, 127.80, 127.25, 123.98, 121.66, 118.47, 117.58, 112.82, 111.25, 110.60, 110.00, 107.10. HPLC analysis: retention time = 22.4 min; peak area, 95.7%.

4.8.7. 2′-Chloro-4′-((2-((4-cyanophenyl)amino)thieno[3,2-d]pyrimidin-4-yl)oxy)-[1,1′-biphenyl]-4-carbonitrile (**20**)

Yield: 90%. mp: 276.7–278.6 °C. ^{1}H NMR (400 MHz, DMSO-d_6) δ: 10.10 (s, 1H), 8.40 (d, J = 5.3 Hz, 1H), 8.00 (d, J = 8.0 Hz, 2H), 7.86 (d, J = 8.4 Hz, 2H), 7.82 (s, 1H), 7.72 (d, J = 8.0 Hz, 2H), 7.65–7.54 (m, 4H), 7.48 (d, J = 5.3 Hz, 1H). ^{13}C NMR (101 MHz, CF_3COOD, $CDCl_3$) δ: 166.28, 151.74, 151.16, 150.75, 143.35, 143.05, 140.18, 133.53, 133.25, 132.71, 132.19, 130.27, 123.71, 121.96, 120.46, 118.55, 117.60, 112.90, 111.56, 110.54, 110.07, 107.44. HPLC analysis: retention time = 22.7 min; peak area, 96.0%.

4.8.8. 4′-((2-((4-Cyanophenyl)amino)thieno[3,2-d]pyrimidin-4-yl)oxy)-3′-(trifluoromethyl)-[1,1′-biphenyl]-4-carbonitrile (**21**)

Yield: 75%. mp: 245.3–247.9 °C. ^{1}H NMR (400 MHz, CF_3COOD, $CDCl_3$) δ: 8.43 (d, J = 5.4 Hz, 1H), 8.14 (s, 1H), 8.04 (d, J = 10.0 Hz, 1H), 7.98 (d, J = 8.3 Hz, 2H), 7.88 (d, J = 8.3 Hz, 2H), 7.61 (d, J = 8.5 Hz, 1H), 7.57 (d, J = 5.4 Hz, 1H), 7.44 (q, J = 8.9 Hz, 4H). ^{13}C NMR (101 MHz, CF_3COOD, $CDCl_3$) δ: 166.45, 151.69, 150.85, 148.51, 143.46, 140.14, 139.43, 133.52, 133.09, 132.03, 127.83, 126.51, 126.46, 124.94, 123.99, 121.83, 117.42, 112.81, 111.55, 110.79, 109.99, 107.25. HRMS (ESI) *m/z* $C_{27}H_{14}F_3N_5OS$: calcd 513.0871, found 514.0940 $[M + H]^+$. HPLC analysis: retention time = 22.1 min; peak area, 97.9%.

4.8.9. 4′-((2-((4-Cyanophenyl)amino)thieno[3,2-d]pyrimidin-4-yl)oxy)-2′-(trifluoromethyl)-[1,1′-biphenyl]-4-carbonitrile (**22**)

Yield: 91%. mp: 244.4–246.2 °C. ^{1}H NMR (400 MHz, CF_3COOD,

$CDCl_3$) δ: 8.39 (d, J = 5.3 Hz, 1H), 7.89 (d, J = 8.0 Hz, 2H), 7.79 (s, 1H), 7.59–7.51 (m, 7H), 7.45 (d, J = 8.4 Hz, 2H). ^{13}C NMR (101 MHz, CF_3COOD, $CDCl_3$) δ: 166.23, 151.88, 150.80, 150.68, 143.65, 143.15, 140.02, 138.68, 133.52, 133.19, 132.42, 130.73, 130.42, 129.81, 123.46, 120.14, 120.09, 118.47, 117.58, 112.82, 111.61, 110.80, 110.00, 107.63. HRMS (ESI) m/z $C_{27}H_{14}F_3N_5OS$: calcd 513.0871, found 514.0943 $[M + H]^+$. HPLC analysis: retention time = 22.4 min; peak area, 96.6%.

*4.8.10. 4-((2-((4-Cyanophenyl)amino)thieno[3,2-d]pyrimidin-4-yl)oxy)-[1,1′-biphenyl]-3,4′-dicarbonitrile (**23**)*

Yield: 88%. mp: > 300 °C. ^{1}H NMR (400 MHz, CF_3COOD, $CDCl_3$) δ: 8.43 (d, J = 5.3 Hz, 1H), 8.11 (d, J = 12.2 Hz, 2H), 7.96 (d, J = 7.9 Hz, 2H), 7.81 (d, J = 8.0 Hz, 2H), 7.67 (d, J = 8.4 Hz, 1H), 7.57 (d, J = 5.3 Hz, 1H), 7.53–7.36 (m, 4H). ^{13}C NMR (101 MHz, CF_3COOD, $CDCl_3$) δ: 165.50, 152.53, 151.86, 151.57, 143.96, 142.23, 139.98, 134.07, 133.71, 133.15, 132.57, 127.84, 124.16, 122.18, 118.49, 117.74, 113.04, 112.84, 111.50, 111.29, 110.01, 107.69, 107.35. HRMS (ESI) m/z $C_{27}H_{14}N_6OS$: calcd 470.0950, found 469.0869 $[M - H]^+$. HPLC analysis: retention time = 22.0 min; peak area, 98.9%.

*4.8.11. 4-((2-((4-Cyanophenyl)amino)thieno[3,2-d]pyrimidin-4-yl)oxy)-[1,1′-biphenyl]-2,4′-dicarbonitrile (**24**)*

Yield: 76%. mp: > 300 °C. ^{1}H NMR (400 MHz, CF_3COOD, $CDCl_3$) δ: 8.43 (d, J = 5.3 Hz, 1H), 8.01 (d, J = 7.9 Hz, 2H), 7.91 (s, 1H), 7.83–7.74 (m, 4H), 7.62–7.55 (m, 3H), 7.48 (d, J = 8.4 Hz, 2H). ^{13}C NMR (101 MHz, CF_3COOD, $CDCl_3$) δ: 165.89, 151.91, 150.98, 150.86, 143.50, 143.20, 141.44, 139.93, 133.36, 133.25, 131.92, 129.44, 127.74, 127.25, 122.39, 118.45, 117.56, 112.81, 112.00, 111.55, 109.99, 107.88. HRMS (ESI) m/z $C_{27}H_{14}N_6OS$: calcd 470.0950, found 471.1014 $[M + H]^+$. HPLC analysis: retention time = 22.6 min; peak area, 96.8%.

*4.8.12. 4′-((2-((4-Cyanophenyl)amino)thieno[3,2-d]pyrimidin-4-yl)oxy)-3′-nitro-[1,1′-biphenyl]-4-carbonitrile (**25**)*

Yield: 92%. mp: 297.5–298.6 °C. ^{1}H NMR (400 MHz, CF_3COOD, $CDCl_3$) δ: 8.55 (d, J = 1.9 Hz, 1H), 8.44 (d, J = 5.4 Hz, 1H), 8.16 (dd, J = 8.4, 2.0 Hz, 1H), 8.00 (d, J = 8.2 Hz, 2H), 7.89 (d, J = 8.3 Hz, 2H), 7.69 (d, J = 8.5 Hz, 1H), 7.57 (d, J = 5.4 Hz, 1H), 7.45 (d, J = 8.6 Hz, 2H), 7.35 (d, J = 8.7 Hz, 2H). ^{13}C NMR (101 MHz, CF_3COOD, $CDCl_3$) δ: 166.09, 151.78, 151.20, 144.18, 143.74, 142.23, 141.31, 140.20, 139.97, 134.07, 133.72, 133.10, 127.83, 125.92, 124.90, 122.20, 118.44, 117.54, 112.80, 111.46, 109.97, 107.53. HRMS (ESI) m/z $C_{26}H_{14}N_6O_3S$: calcd 490.0848, found 491.0923 $[M + H]^+$. HPLC analysis: retention time = 21.3 min; peak area, 95.3%.

*4.8.13. 4′-((2-((4-Cyanophenyl)amino)thieno[3,2-d]pyrimidin-4-yl)oxy)-2′-nitro-[1,1′-biphenyl]-4-carbonitrile (**26**)*

Yield: 79%. mp: 255.8–257.7 °C. ^{1}H NMR (400 MHz, DMSO-d_6) δ: 10.11 (s, 1H), 8.42 (d, J = 5.3 Hz, 1H), 8.29 (s, 1H), 8.00 (d, J = 8.2 Hz, 2H), 7.93 (d, J = 10.6 Hz, 1H), 7.84 (d, J = 8.6 Hz, 2H), 7.78 (d, J = 8.4 Hz, 1H), 7.65 (d, J = 8.1 Hz, 2H), 7.59 (d, J = 8.6 Hz, 2H), 7.50 (d, J = 5.3 Hz, 1H). ^{13}C NMR (101 MHz, DMSO-d_6) δ: 165.06, 163.73, 157.07, 152.48, 149.25, 145.27, 141.77, 138.40, 133.63, 133.24, 133.21, 131.81, 129.55, 127.80, 123.86, 119.99, 119.24, 118.96, 118.81, 111.75, 109.71, 102.83. HRMS (ESI) m/z $C_{26}H_{14}N_6O_3S$: calcd 490.0848, found 491.0917 $[M + H]^+$. HPLC analysis: retention time = 22.6 min; peak area, 96.5%.

*4.8.14. 4′-((2-((4-Cyanophenyl)amino)thieno[3,2-d]pyrimidin-4-yl)oxy)-2′-methoxy-[1,1′-biphenyl]-4-carbonitrile (**27**)*

Yield: 80%. mp: 280.0–282.0 °C. ^{1}H NMR (400 MHz, DMSO-d_6) δ: 10.07 (s, 1H), 8.37 (d, J = 5.3 Hz, 1H), 8.04–7.92 (m, 5H), 7.76 (d, J = 8.4 Hz, 2H), 7.62 (s, 1H), 7.51–7.43 (m, 4H), 3.85 (s, 3H). ^{13}C NMR (101 MHz, CF_3COOD, $CDCl_3$) δ: 166.56, 151.45, 151.17, 150.43, 145.32, 142.58, 140.82, 140.53, 140.16, 133.35, 133.12, 128.12, 127.86, 123.03, 121.20, 120.34, 118.43, 117.43, 112.79, 111.73, 111.39, 110.02, 109.96, 106.72, 55.95. HRMS (ESI) m/z $C_{27}H_{17}N_5O_2S$: calcd 475.1103, found 476.1166 $[M + H]^+$. HPLC analysis: retention time = 22.0 min; peak area, 97.0%.

*4.8.15. 4′-((2-((4-Cyanophenyl)amino)thieno[3,2-d]pyrimidin-4-yl)oxy)-3′-methoxy-[1,1′-biphenyl]-4-carbonitrile (**28**)*

Yield: 71%. mp: 214.9–216.2 °C. ^{1}H NMR (400 MHz, CF_3COOD, $CDCl_3$) δ: 8.41 (d, J = 5.2 Hz, 1H), 7.91 (d, J = 7.9 Hz, 2H), 7.82 (d, J = 7.9 Hz, 2H), 7.64–7.47 (m, 6H), 7.09 (d, J = 8.3 Hz, 1H), 7.04 (s, 1H), 3.89 (s, 3H). ^{13}C NMR (101 MHz, CF_3COOD, $CDCl_3$) δ: 166.82, 157.83, 152.47, 151.57, 150.45, 142.89, 142.73, 140.39, 133.20, 132.46, 131.59, 130.20, 128.26, 121.42, 118.45, 117.42, 113.87, 112.80, 111.66, 109.98, 109.26, 106.98, 105.45, 55.66. HRMS (ESI) m/z $C_{27}H_{17}N_5O_2S$: calcd 475.1103, found 476.1164 $[M + H]^+$. HPLC analysis: retention time = 22.2 min; peak area, 97.9%.

*4.8.16. 4′-((2-((4-Cyanophenyl)amino)thieno[3,2-d]pyrimidin-4-yl)oxy)-3′,5′-dimethyl-[1,1′-biphenyl]-4-carbonitrile (**29**)*

Yield: 93%. mp: 287.1–288.5 °C. ^{1}H NMR (400 MHz, CF_3COOD, $CDCl_3$) δ: 8.37 (d, J = 5.0 Hz, 1H), 7.90 (d, J = 8.2 Hz, 2H), 7.82 (d, J = 8.2 Hz, 2H), 7.55 (d, J = 5.1 Hz, 1H), 7.52 (s, 2H), 7.34 (s, 4H), 2.28 (s, 6H). ^{13}C NMR (101 MHz, CF_3COOD, $CDCl_3$) δ: 166.00, 151.59, 150.79, 149.74, 145.24, 142.73, 140.45, 138.51, 133.28, 133.17, 131.12, 128.15, 127.77, 120.96, 118.63, 117.84, 112.97, 110.82, 110.14, 106.98, 15.99. HRMS (ESI) m/z $C_{28}H_{19}N_5OS$: calcd 473.1310, found 474.1376 $[M + H]^+$. HPLC analysis: retention time = 22.8 min; peak area, 95.0%.

*4.8.17. 4′-((2-((4-Cyanophenyl)amino)thieno[3,2-d]pyrimidin-4-yl)oxy)-2′,3′-difluoro-[1,1′-biphenyl]-4-carbonitrile (**30**)*

Yield: 86%. mp: 279.0–280.7 °C. ^{1}H NMR (400 MHz, DMSO-d_6) δ: 10.14 (s, 1H), 8.46 (d, J = 4.9 Hz, 1H), 8.05 (d, J = 7.8 Hz, 2H), 7.90–7.84 (m, 4H), 7.63–7.58 (m, 4H), 7.53 (d, J = 5.0 Hz, 1H). ^{13}C NMR (101 MHz, CF_3COOD, $CDCl_3$) δ: 165.50, 151.50 (d, J = 89.4 Hz, 1C), 141.71, 138.94, 133.11, 133.08, 129.52, 129.49, 124.64, 122.43, 118.42, 118.32, 117.49, 112.78, 110.91, 109.96, 107.65. HRMS (ESI) m/z $C_{26}H_{13}F_2N_5OS$: calcd 481.0809, found 482.0884 $[M + H]^+$. HPLC analysis: retention time = 22.4 min; peak area, 98.5%.

*4.8.18. 4′-((2-((4-Cyanophenyl)amino)thieno[3,2-d]pyrimidin-4-yl)oxy)-3′,5′-difluoro-[1,1′-biphenyl]-4-carbonitrile (**31**)*

Yield: 82%. mp: > 300 °C. ^{1}H NMR (400 MHz, DMSO-d_6) δ: 10.17 (s, 1H), 8.46 (d, J = 5.3 Hz, 1H), 8.05 (d, J = 8.2 Hz, 2H), 7.99 (d, J = 8.2 Hz, 2H), 7.90 (d, J = 9.3 Hz, 2H), 7.78 (d, J = 8.5 Hz, 2H), 7.58–7.48 (m, 3H). ^{13}C NMR (101 MHz, CF_3COOD, $CDCl_3$) δ: 165.25, 155.04, 151.86, 151.30, 143.68, 142.81, 140.23, 140.08, 133.59, 133.19, 133.13, 127.67, 122.08, 118.45, 117.61, 112.80, 111.49, 111.25, 111.04, 109.98, 107.47. HRMS (ESI) m/z $C_{26}H_{13}F_2N_5OS$: calcd 481.0809, found 482.0874 $[M + H]^+$. HPLC analysis: retention time = 22.5 min; peak area, 98.8%.

*4.8.19. 3′-Chloro-4′-((2-((4-cyanophenyl)amino)thieno[3,2-d]pyrimidin-4-yl)oxy)-5′-methyl-[1,1′-biphenyl]-4-carbonitrile (**32**)*

Yield: 76%. mp: > 300 °C. ^{1}H NMR (400 MHz, CF_3COOD, $CDCl_3$) δ: 8.41 (d, J = 5.4 Hz, 1H), 7.93 (d, J = 8.2 Hz, 2H), 7.81 (d, J = 8.2 Hz, 2H), 7.73 (s, 1H), 7.57 (d, J = 5.7 Hz, 2H), 7.39 (s, 4H), 2.37 (s, 3H). ^{13}C NMR (101 MHz, CF_3COOD, $CDCl_3$) δ: 165.55, 151.64, 151.02, 146.65, 143.88, 143.16, 140.28, 139.60, 133.58, 133.44, 133.12, 128.78, 127.78, 126.87, 121.46, 118.48, 117.73, 112.83, 110.98, 110.48, 110.01, 107.08, 16.13. HRMS (ESI) m/z $C_{27}H_{16}ClN_5OS$: calcd 493.0764, found 494.0827 $[M + H]^+$. HPLC analysis: retention time = 22.7 min; peak area, 96.9%.

4.9. Antiviral activity assays

4.9.1. In vitro anti-HIV assay

The anti-HIV activity of the compounds was evaluated against WT HIV-1 (HIV-IIIB strain), single- and double- mutant strains (L100I, K103N, E138K, Y181C, Y188L, K103N + Y181C (RES056) and F227L + V106A), in MT-4 cell cultures using the method of 3-(4,5-dimethylthiazol-2-yl)-2,5-diphenyltetrazolium bromide (MTT). Briefly, virus stocks were titrated in MT-4 cells and expressed as the 50% cell culture infective dose (CCID50). MT-4 cells were suspended in culture medium at 1×10^5 cells/mL and infected with HIV at a multiplicity of infection of 0.02. Immediately after viral infection,100 mL of the cell suspension was placed in each well of a flat-bottomed micro-titer tray containing various concentrations of the test compounds. The test compounds were dissolved in DMSO at 50 mM or higher. After 4 days of incubation at 37 °C, the number of viable cells was determined using the MTT method. Compounds were tested in parallel for cytotoxic effects in uninfected MT-4 cells.

4.9.2. HIV-1 RT inhibition assay

Recombinant wild type p66/p51 HIV-1 RT was expressed and purified as previously described. The RT assay was performed with the EnzCheck Reverse Transcriptase Assay kit (Molecular Probes, Invitrogen), as described by the Manufacturer. The assay was based on the dsDNA quantitation reagent Pico-Green. This reagent showed a pronounced increase in fluorescence signal upon binding to dsDNA or RNA-DNA hetero-duplexes. Single-stranded nucleic acids generated only minor fluorescence signal enhancement when a sufficiently high dye: base pair ratio was applied. This condition was met in the assay.

A poly(rA) template of approximately 350 bases long and an oligo (dT)16 primer were annealed in a molar ratio of 1:1.2 (60 min, at room temperature). 52 ng of the RNA/DNA was brought into each well of a 96-well plate in a volume of 20 mL polymerization buffer (60 mM Trise HCl, 60 mM KCl, 8 mM $MgCl_2$, 13 mM DTT, 100 mM dTTP, pH = 8.1). 5.0 mL of RT enzyme solution, diluted to a suitable concentration in an enzyme dilution buffer (50 mM Trise-HCl, 20% glycerol, 2 mM DTT, pH = 7.6), was added. The reaction mixture was incubated at 25 °C for 40 min and then stopped by the addition of EDTA (15 mM). Hetero duplexes were then detected by addition of Pico-Green. Signals were read using an excitation wavelength of 490 nm and emission detection at 523 nm using a spectrofluorometer (Safire 2, Tecan). To test the biological activity of compounds against RT, 1.0 mL of compound in DMSO was added to each well before the addition of RT enzyme solution. Control wells without compound contained the same amount of DMSO. Results were expressed as relative fluorescence, i.e. the fluorescence signal of the reaction mixed with compound divided by the signal of the same reaction mixed without compound.

4.10. Molecular modeling

Molecular modelling research work was performed with the Tripos molecular modelling software packages (Sybyl-X 2.0). All the molecules for docking analysis were built using the standard bond lengths and angles from Sybyl-X 2.0/base Builder before being optimized using the Tripos force field for 10,000 generations two times or more, until the minimized conformers of the ligand were the same. The flexible docking method, called Surflex-Dock, docks the ligand automatically into the ligand binding site of the receptor by using a protocol-based approach and an empirically-derived scoring function. The protocol is a computational representation of a putative ligand that binds to the intended binding site and is a unique and essential element of the docking algorithm. The scoring function in Surflex-Dock, which contains hydrophobic, polar, repulsive, entropic, and solvation terms, was trained to estimate the dissociation constant (K_d) expressed in -log $(K_d)^2$. The scoring function in Surflex-Dock, which contains hydrophobic, polar, repulsive, entropic and solvation terms, was trained to estimate the binding energy. Prior to docking, the protein was prepared by removing water molecules, the ligand ETV, and other unnecessary small molecules from the crystal structure of the HIV-1 RT complex [18]. Simultaneously, hydrogen atoms were added to the protein. Surflex-Dock default settings were used for other parameters, such as the number of starting conformations per molecule (set to 0), the size to expand search grid (set to 8 Å), the maximum number of the rotatable bonds per molecule (set to 100), and the maximum number of poses per ligand (set to 20). During the docking procedure, all of the single bonds in amino acid residue side-chains inside the defined RT binding pocket were regarded as rotatable or flexible, and the ligand was allowed to rotate at all single bonds and move flexibly within the tentative binding pocket. The atomic charges were recalculated using the Kollman all-atom approach for the protein and the Gasteiger-Hückel approach for the ligand. The binding interaction energy was calculated, including van der Waals, electrostatic, and torsional energy terms defined in the Tripos force field. The structure optimization was performed for more than 10,000 generations using a genetic algorithm, and the 20-best-scoring ligand-protein complexes were kept for the further analyses. The -log$(K_d)^2$ values of the 20-best-scoring complexes, which represented the binding affinities of the ligand with RT, encompassed a wide scope of the functional classes (10^{-2}–10^{-9}). Only the highest scoring 3D structural model of the ligand-bound RT was chosen to define the binding interaction.

Acknowledgements

We gratefully acknowledge the generous support provided by National Natural Science Foundation of P.R. China under Grant No. 21372050, and Shanghai Municipal Natural Science Foundation under Grant No. 13ZR1402200.

We thank K. Erven, K. Uyttersprot, and C. Heens for technical assistance with the HIV assays.

Appendix A. Supplementary material

Supplementary data to this article can be found online at https://doi.org/10.1016/j.bioorg.2019.102974.

References

[1] Y.H. Liang, X.Q. Feng, Z.S. Zeng, F.E. Chen, J. Balzarini, C. Pannecouque, E. De Clercq, Design, synthesis, and SAR of naphthyl-substituted Diarylpyrimidines as non-nucleoside inhibitors of HIV-1 reverse transcriptase, ChemMedChem 4 (2009) 1537–1545.

[2] S.X. Gu, Z.M. Li, X.D. Ma, S.Q. Yang, Q.Q. He, F.E. Chen, E. De Clercq, J. Balzarini, C. Pannecouque, Chiral resolution, absolute configuration assignment and biological activity of racemic diarylpyrimidine CH(OH)-DAPY as potent nonnucleoside HIV-1 reverse transcriptase inhibitors, Eur. J. Med. Chem. 53 (2012) 229–234.

[3] Z.Y. Wan, J. Yao, T.Q. Mao, X.L. Wang, H.F. Wang, W.X. Chen, H. Yin, F.E. Chen, E. De Clercq, D. Daelemans, C. Pannecouque, Pyrimidine sulfonylacetanilides with improved potency against key mutant viruses of HIV-1 by specific targeting of a highly conserved residue, Eur. J. Med. Chem. 102 (2015) 215–222.

[4] Z.Y. Wan, J. Yao, Y. Tao, T.Q. Mao, X.L. Wang, Y.P. Lu, H.F. Wang, H. Yin, Y. Wu, F.E. Chen, E. De Clercq, D. Daelemans, C. Pannecouque, Discovery of piperidin-4-yl-aminopyrimidine derivatives as potent non-nucleoside HIV-1 reverse transcriptase inhibitors, Eur. J. Med. Chem. 97 (2015) 1–9.

[5] L. Ji, F.E. Chen, E. De Clercq, J. Balzarini, C. Pannecouque, Synthesis and anti-HIV-1 activity evaluation of 5-alkyl-2-alkylthio-6-(arylcarbonyl or alpha-cyanoarylmethyl)-3,4-dihydropyrimidin-4(3H)-ones as novel non-nucleoside HIV-1 reverse transcriptase inhibitors, J. Med. Chem. 50 (2007) 1778–1786.

[6] K. Jin, H. Yin, E. De Clercq, C. Pannecouque, G. Meng, F. Chen, Discovery of biphenyl-substituted diarylpyrimidines as non-nucleoside reverse transcriptase inhibitors with high potency against wild-type and mutant HIV-1, Eur. J. Med. Chem. 145 (2018) 726–734.

[7] S.K. Vernekar, Z. Liu, E. Nagy, L. Miller, K.A. Kirby, D.J. Wilson, J. Kankanala, S.G. Sarafianos, M.A. Parniak, Z. Wang, Design, synthesis, biochemical, and antiviral evaluations of C6 benzyl and C6 biarylmethyl substituted 2-hydroxylisoquinoline-1,3-diones: dual inhibition against HIV reverse transcriptase-associated RNase H and polymerase with antiviral activities, J. Med. Chem. 58 (2015) 651–664.

[8] J. Guillemont, E. Pasquier, P. Palandjian, D. Vernier, S. Gaurrand, P.J. Lewi, J. Heeres, M.R. de Jonge, L.M. Koymans, F.F. Daeyaert, M.H. Vinkers, E. Arnold,

K. Das, R. Pauwels, K. Andries, M.P. de Bethune, E. Bettens, K. Hertogs, P. Wigerinck, P. Timmerman, P.A. Janssen, Synthesis of novel diarylpyrimidine analogues and their antiviral activity against human immunodeficiency virus type 1, J. Med. Chem. 48 (2005) 2072–2079.

[9] Z. Zhou, T. Liu, D. Kang, Z. Huo, G. Wu, D. Daelemans, E. De Clercq, C. Pannecouque, P. Zhan, X. Liu, Discovery of novel diarylpyrimidines as potent HIV-1 NNRTIs by investigating the chemical space of a less explored "hydrophobic channel", Org. Biomol. Chem. 16 (2018) 1014–1028.

[10] D. Kang, Z. Fang, B. Huang, X. Lu, H. Zhang, H. Xu, Z. Huo, Z. Zhou, Z. Yu, Q. Meng, G. Wu, X. Ding, Y. Tian, D. Daelemans, E. De Clercq, C. Pannecouque, P. Zhan, X. Liu, Structure-based optimization of thiophene[3,2-*d*]pyrimidine derivatives as potent HIV-1 non-nucleoside reverse transcriptase inhibitors with improved potency against resistance-associated variants, J. Med. Chem. 60 (2017) 4424–4443.

[11] D. Kang, Z. Fang, Z. Li, B. Huang, H. Zhang, X. Lu, H. Xu, Z. Zhou, X. Ding, D. Daelemans, E. De Clercq, C. Pannecouque, P. Zhan, X. Liu, Design, synthesis, and evaluation of thiophene[3,2-d]pyrimidine derivatives as HIV-1 non-nucleoside reverse transcriptase inhibitors with significantly improved drug resistance profiles, J. Med. Chem. 59 (2016) 7991–8007.

[12] Z.S. Zeng, Q.Q. He, Y.H. Liang, X.Q. Feng, F.E. Chen, E. De Clercq, J. Balzarini, C. Pannecouque, Hybrid diarylbenzopyrimidine non-nucleoside reverse transcriptase inhibitors as promising new leads for improved anti-HIV-1 chemotherapy, Bioorg. Med. Chem. 18 (2010) 5039–5047.

[13] D. Li, P. Zhan, E. De Clercq, X. Liu, Strategies for the design of HIV-1 non-nucleoside reverse transcriptase inhibitors: lessons from the development of seven representative paradigms, J. Med. Chem. 55 (2012) 3595–3613.

[14] V. Namasivayam, M. Vanangamudi, V.G. Kramer, S. Kurup, P. Zhan, X. Liu, J. Kongsted, S.N. Byrareddy, The journey of HIV-1 non-nucleoside reverse transcriptase inhibitors (NNRTIs) from lab to clinic, J. Med. Chem. (2018), https://doi.org/10.1021/acs.jmedchem.8b00843.

[15] K.A. Paris, O. Haq, A.K. Felts, K. Das, E. Arnold, R.M. Levy, Conformational landscape of the human immunodeficiency virus type 1 reverse transcriptase non-nucleoside inhibitor binding pocket: lessons for inhibitor design from a cluster analysis of many crystal structures, J. Med. Chem. 52 (2009) 6413–6420.

[16] C. Dousson, F.R. Alexandre, A. Amador, S. Bonaric, S. Bot, C. Caillet, T. Convard, D. da Costa, M.P. Lioure, A. Roland, E. Rosinovsky, S. Maldonado, C. Parsy, C. Trochet, R. Storer, A. Stewart, J. Wang, B.A. Mayes, C. Musiu, B. Poddesu, L. Vargiu, M. Liuzzi, A. Moussa, J. Jakubik, L. Hubbard, M. Seifer, D. Standring, Discovery of the aryl-phospho-indole IDX899, a highly potent anti-HIV non-nucleoside reverse transcriptase inhibitor, J. Med. Chem. 59 (2016) 1891–1898.

[17] Y. Yang, D. Kang, L.A. Nguyen, Z.B. Smithline, C. Pannecouque, P. Zhan, X. Liu, T.A. Steitz, Structural basis for potent and broad inhibition of HIV-1 RT by thiophene[3,2-d]pyrimidine non-nucleoside inhibitors, eLife 7 (2018) e36340.

[18] E.B. Lansdon, K.M. Brendza, M. Hung, R. Wang, S. Mukund, D. Jin, G. Birkus, N. Kutty, X. Liu, Crystal structures of HIV-1 reverse transcriptase with etravirine (TMC125) and rilpivirine (TMC278): implications for drug design, J. Med. Chem. 53 (2010) 4295–4299.